Optimizing the definition of a sudden stratospheric warming

Amy H. Butler[1,2] and Edwin P. Gerber[3]

[1]Cooperative Institute for Research in Environmental Sciences/University of Colorado-Boulder, Boulder, CO, USA
[2]National Oceanic and Atmospheric Administration, Earth System Research Laboratory, Chemical Sciences Division, Boulder, CO, USA
[3]Courant Institute of Mathematical Sciences, New York University, New York, NY, USA

Corresponding author: Amy Butler, amy.butler@noaa.gov

Submitted to Journal of Climate

Abstract

Various criteria exist for determining the occurrence of a major sudden stratospheric warming (SSW), but the most common is based on the reversal of the climatological westerly zonal-mean zonal winds at 60° latitude and 10 hPa in the winter stratosphere. This definition was established at a time when observations of the stratosphere were sparse, and chosen in part simply because winds here could be measured. Given greater access to data in the satellite era, a systematic analysis of the optimal parameters of latitude, altitude, and threshold for the wind reversal is now possible. Here, the frequency of SSWs, the strength of the wave forcing associated with the events, changes in stratospheric temperature and zonal winds, and surface impacts are examined as a function of the stratospheric wind reversal parameters. The results provide a methodical assessment of how to best define a “standard” metric for major SSWs. While the continuum nature of stratospheric variability makes it difficult to identify a decisively optimal threshold, there is a relatively narrow envelope of thresholds that work well — and the original focus at 60° latitude and 10 hPa lies within this window.

1. Introduction

In the decades following the first observations of a major sudden stratospheric warming (SSW) by Scherhag (1952), various metrics were developed to classify extreme events in the stratosphere (Butler et al. 2015). During a SSW, the winter stratosphere rapidly warms and the climatological westerly polar vortex decelerates, often reversing entirely. Thus the earliest SSW definitions adopted by the World Meteorological Organization (WMO) focused on temperature gradient and zonal wind reversals at the 10 hPa pressure level (~30 km), and poleward of 60° latitude (WMO/IQSY 1964; Quiroz et al. 1975; WMO CAS 1978; McInturff 1978; Labitzke 1981). The initial focus on 10 hPa and 60°N arose from careful synoptic analysis of where the greatest changes were being observed during these events. It was also informed by the availability of data; most of the earliest observations were taken by radiosondes and rocketsondes equatorward of 60°N over Northern Hemisphere (NH) mid-latitude land regions (Johnson et al. 1969). Today the most commonly used definition for SSWs still relies on the zonal-mean zonal wind reversal at 60° latitude and 10 hPa (Charlton & Polvani 2007).

Recent work has shown, however, that the classification of major SSWs by this simple zonal wind definition is sensitive to the choice of latitude, pressure level, and threshold used to detect the events (Butler et al. 2015; Palmeiro et al. 2015). Various other techniques, including annular modes (Baldwin 2001; Baldwin & Thompson 2009; Gerber et al. 2010), geometric vortex diagnostics (Waugh & Randel 1999; Hannachi et al. 2011; Mitchell et al. 2011; Seviour et al. 2013), deceleration based measures (Kim et al. 2017), temperature changes (Blume et al. 2012; Maury et al. 2016), and empirical orthogonal functions (EOF) (Hitchcock et al. 2013) have also been used to detect extreme polar vortex events. These too ultimately rely on arbitrary thresholds, are sensitive to the parameters chosen, and can be more computationally intensive.

Given the sizable increase in measurements of the middle atmosphere since the satellite-era began, we conduct a systematic evaluation of where a zonal wind reversal should be defined in order to "optimize" the classification of major SSWs. The detection algorithm should, first and foremost, isolate events that are (1) sudden: a rapid deceleration of the stratospheric polar vortex, and (2) warming: a large amplitude temperature increase. Ideally, the definition will also capture events with significant two-way coupling between the troposphere and stratosphere, maximizing (3) the upward wave propagation into the stratosphere prior to events and (4) the downward coupling of the zonal mean circulation to the surface after events. After presenting our methodology in Section 2, we show where metrics (1)-(4) are optimized in relation to pressure level, latitude, and threshold of the zonal wind reversal in Section 3. We also consider how the frequency of events changes in response to parameters. Our conclusions are presented in Section 4.

2. Methodology

A commonly used definition for major mid-winter SSWs is a reversal of the zonal-mean zonal winds at 60°N and 10 hPa during the months of November-March (Charlton and Polvani 2007, hereafter CP07). Here, reversals are separated by at least 20 consecutive days of westerlies to ensure events are independent, and westerlies must return for at least 10 consecutive days prior to April 30th to avoid including final warmings. Disadvantages of this definition are that, by construction, it does not detect final warmings, and the April 30th requirement is an arbitrary cut-off. We address these with minor changes to the CP07 method.

We extend the analysis from July 1st to June 30th of the following year, and first detect the start and end of the vortex for each year. The start occurs when westerlies persist for at least 10 consecutive days. The end of the vortex, or final warming (FW), occurs on the last date when the winds reverse and do not return to westerly for more than 10 consecutive days. The FWs at 60°N and 10 hPa detected with this method agree well with FW dates from Hu et al. (2015) (**Supplementary Table 1**), while maintaining consistency with the major SSW definition.

SSWs are then detected by reversals during this extended winter season, but with a more stringent requirement that zonal wind reversals be separated by 30 consecutive days of westerlies. A 20-day separation, however, does not significantly change our results. **Table 1** compares our SSW dates based on zonal wind reversal at 60° latitude and 10 hPa with CP07. Only three events, all in March, are classified as mid-winter SSWs by CP07 but not by our method. One of these events (14-Mar-88) is found to be a final warming; the other two dates are not separated from earlier SSW dates by at least 30 consecutive days of westerlies. (**See supplementary Figure 1.**)

Using these separation and final warming criteria, we examine how the dates and synoptic properties of SSWs vary with the latitude and level at which the zonal wind is measured, and with the threshold of deceleration. Here, the "threshold" sets the magnitude to which the vortex winds must decelerate to count as a major event. It has traditionally been defined at 0 $m\ s^{-1}$ because planetary waves cannot further propagate into easterly flow (Charney & Drazin 1961). For event separation, with negative thresholds ($u_c <= 0\ m\ s^{-1}$) the winds must return to westerly ($u > 0$ m s^{-1}) for at least 30 consecutive days, while with positive thresholds ($u_c > 0$ m s^{-1}), the winds must exceed u_c for at least 30 consecutive days after the event.

We use daily-mean output of JRA-55 reanalysis from 1958-2016 (Ebita et al. 2011), but the results are robust to the choice of reanalysis. For assessing the synoptic behavior surrounding events, daily anomalies are calculated relative to a smooth annual cycle, computed by averaging each calendar day over the entire period, and then filtering in Fourier space by retaining only the first four harmonics. For the Arctic Oscillation (AO) index, we use daily historical values provided by the National Centers for Environmental Prediction (NCEP) Climate Prediction Center (CPC), which are based on EOF analysis of the 1000 hPa geopotential height anomalies from the NCEP/NCAR reanalysis data and standardized by the DJFM (Dec-Mar) daily values.

The mean of each synoptic property in **Section 3** is found by averaging over all events determined at a given location and threshold. Significance testing is performed via a Monte Carlo test, in which we repeatedly sample the same day and month of events for a particular set of parameters, but randomize the years 500 times. We then determine if the difference in means between the two distributions (assuming unequal variances) exceeds the 95% *t*-test. In most cases, the signals are significantly different everywhere. If less than 2 SSWs per decade (i.e., less than 12 SSWs from 1958-2016) are detected at a given location, the metric is assigned a missing value.

3. Optimizing the SSW definition

CP07 and Charlton et al. (2007) propose several key metrics for evaluating major SSWs in model simulations (c.f., CP07 Table 3). Here, we consider many of the same properties, but apply them to zonal wind decelerations everywhere between 50 hPa to 1 hPa, 50°N to 80°N, and for thresholds of -10 to 10 m s^{-1}. **Figure 1** shows how two fundamental synoptic characteristics of SSWs, the suddenness of the vortex breakdown and the magnitude of the temperature increase, vary depending on the location and threshold of the "reversal".

"Suddenness" is characterized by the change in the 10 hPa 60°N zonal-mean zonal wind, computed from the mean of days 0-5 *after* the event minus days 5-15 *prior* to each event (**Fig 1a, b**). While the vortex must decelerate in all cases to trigger an event, large values here indicate that the deceleration was rapid. For example, at 60°N and 10 hPa (**Figure 1a**, black dot), the value is -30 m s^{-1}: this indicates for events defined by a reversal at this location (as in CP07), the vortex abruptly slows by 30 m s^{-1} in approximately 10 days. If, for example, one defines events by a reversal at 70°N and 10 hPa, the average deceleration is weaker, approximately -24 m s^{-1}. Overall, we find that the most abrupt events are found when the zonal wind reverses along the equatorward vortex edge, maximized from 20 hPa to 7 hPa as one moves from ~62.5° to 57.5°N. **Figure 1b** shows that if we fix the pressure level at which events are defined at 10 hPa, requiring a stronger threshold (i.e. less than -2 m s^{-1}) selects the strongest events with greater deceleration. This is partly by construction; a negative threshold will capture fewer, stronger events. Note that qualitatively similar results are found if one quantifies the deceleration at 65°N or 70°N instead of 60°N.

The "warming" metric (**Fig 1c, d**) is defined as the 10 hPa polar cap (50-90°N) temperature anomaly for the mean of days -5 to +5 around each event. It is also maximized for zonal wind reversals that occur on the equatorward edge of the polar vortex (50-65°N), though values are largest for reversals from 10 hPa to 1 hPa. As before, requiring a more negative threshold at 10 hPa (**Fig 1d**) selects events with larger temperature increases at every latitude. Note, however, that for events at 60°N with thresholds near +1-3 m s^{-1}, both the suddenness and the temperature increase have similar magnitudes as the events with 0 to -3 m s^{-1} thresholds. This similarity suggests that wind decelerations that nearly reach 0 m s^{-1}, but don't actually reverse the polar vortex, are still associated with substantial dynamic changes in the stratosphere.

Figure 2 considers two additional desirable properties of major SSWs: upward and downward coupling between the troposphere and the stratosphere. Upward wave propagation from the troposphere is represented by the 45-75°N eddy heat flux (v'T') anomalies at 100 hPa, averaged from days -20 to 0 of each event (**Fig 2a**). Reversals occurring equatorward of 65°N and at pressure levels greater than 10 hPa are associated with stronger poleward (positive) eddy heat flux anomalies prior to the event, indicating that stronger wave driving is necessary to reverse the zonal wind here. Note that there are also fewer reversals that occur here (**Figure 3**). Stronger heat flux anomalies are also associated with reversals below the 0 m s^{-1} threshold (**Fig 2b**).

The strength of the stratospheric coupling to the surface is characterized by the mean Arctic Oscillation (AO) daily index for days 0-60 after events (**Fig 2c, d**). The AO is the dominant mode of climate variability in the NH mid-latitudes; a weakening of the polar vortex is associated with the negative phase of the AO, i.e. an equatorward shift of the tropospheric storm track. It is clear that reversals in the *lower* stratosphere between 60-70°N result in the largest impacts on the AO (**Fig 2c**), in agreement with previous studies (Gerber et al. 2009; Hitchcock & Simpson

2014; Maycock & Hitchcock 2015; Karpechko et al. 2017). Similar results are found for a metric based on Eurasian surface temperature anomalies (not shown). For decelerations at 10 hPa (**Fig 2d**), AO impacts are not strongly dependent on threshold, though the largest changes occur for negative thresholds between 60-70°N. Comparing the top and bottom rows of **Figure 2**, it is seen that wind decelerations with the strongest upward wave driving are not always associated with the strongest influence on the surface.

The frequency of events is quite sensitive to where the zonal wind deceleration is defined (**Figure 3**; see also Butler et al. 2015). At pressure levels higher than ~10 hPa, the number of zonal wind reversals per decade increases primarily with latitude; at pressure levels less than 10 hPa, the frequency is primarily a function of height (**Fig 3a**). Note that regions that have similar SSW frequency aren't necessarily detecting the same events. **Figure 3c** shows the percent match[1] of events within +/- 10 days of CP07 SSW events (i.e., reversals at 10 hPa and 60°N). Zonal wind reversals along the edge of the polar vortex detect greater than 50% of the same events (solid black contour), though similarities greater than 80% are uncommon.

The frequency of events decreases if the threshold value is more negative, particularly equatorward of 65°N (**Fig 3b**). While more events are detected as the critical threshold is relaxed to more positive values, these events also have weaker dynamic impacts overall (**Figs 1 and 2**). The agreement of dates with those at 0 m s^{-1} and 10 hPa and 60°N is greater than 50% for a broad range of different thresholds; in particular, as the required threshold becomes more

[1] Percent match is calculated here as P = A/N * 100, where A is the number of same events detected at both 10 hPa and 60°N and a particular location, and N=A+B+C where B is the number of events detected at 10 hPa and 60°N but not the other location, and C is the number of events detected at the particular location but not at 10 hPa and 60°N.

negative, one needs to use decelerations at more poleward locations to detect the same events.

4. Discussion and Conclusions

To summarize these findings, we create a qualitative “score” ranging from 0-1 for each of the four key SSW properties (**Figs 1 and 2**) by dividing the value of each property at a particular location/threshold by the maximum value observed over all locations/thresholds. A score of 1 then implies the optimal location for a given property. **Figure 4** shows the average scores, giving equal weight to each property. While it is somewhat arbitrary to equally weight each evaluation, the scores are not heavily dominated by any one metric. We find that the key properties for SSWs are maximized (average scores > 0.8) for reversals on the equatorward edge of the polar vortex between 55-65°N and in the mid-stratosphere from 30 to 7 hPa (**Fig 4a**) and for reversals near or below 0 m s^{-1} (**Fig 4b**). Choosing different reasonable metrics, or removing one of these metrics, does not qualitatively change this result, though the AO metric tend to depress the scores on events characterized at upper levels.

There is a fairly narrow range of pressure levels, latitudes, and thresholds where features relevant to major SSWs are maximized, and for which there is still a reasonable number of events. Zonal wind reversals at 10 hPa and 60°N fall within this region, indicating that the historically-used definition does detect SSWs with a strong dynamic response in the stratosphere and strong coupling to the troposphere; this is a testament to the synoptic intuition of meteorologists in the pre-satellite era. Our results also suggest that while zonal wind decelerations near 0 m s^{-1} have similar impacts to true wind reversals, there is a decline in stratospheric and tropospheric impacts as the threshold is relaxed to more positive values. The continuum nature of these impacts means that defining SSWs will always involve some degree of subjectivity (e.g., Coughlin & Gray 2009).

There are recent and ongoing efforts to re-evaluate and improve the standard definition for SSWs as defined by the WMO (Butler et al. 2014; Butler et al. 2015). While our analysis lends evidence that major changes to the current definition are unwarranted, there are still potential avenues for improvement. These include clarity of the separation criteria and the inclusion of minor and final warmings consistent with the major warming definition.

Acknowledgments

E.P. Gerber was supported by NSF (AGS-1546585).

References

Baldwin, M.P., 2001. Annular modes in global daily surface pressure. *Geophysical Research Letters*, 28(21), 4115–4118. doi: 10.1029/2001GL013564.

Baldwin, M.P. & Thompson, D.W.J., 2009. A critical comparison of stratosphere-troposphere coupling indices. *Quarterly Journal of the Royal Meteorological Society*, 135(644), 1661–1672. doi: 10.1002/qj.479.

Blume, C., Matthes, K. & Horenko, I., 2012. Supervised Learning Approaches to Classify Sudden Stratospheric Warming Events. *Journal of the Atmospheric Sciences*, 69(6), 1824–1840. doi: 10.1175/JAS-D-11-0194.1.

Butler, A.H., Gerber, E.P., Mitchell, D. & Seviour, W.J.M., 2014. New efforts in developing a standard definition for sudden stratospheric warmings. *SPARC Newsletter*, 43, 23–24.

Butler, A.H., Seidel, D.J., Hardiman, S.C., Butchart, N., Birner, T. & Match, A., 2015. Defining Sudden Stratospheric Warmings. *Bulletin of the American Meteorological Society*, 96(11), 1913–1928. doi: 10.1175/BAMS-D-13-00173.1.

Charlton, A.J. & Polvani, L.M., 2007. A new look at stratospheric sudden warmings. Part I: Climatology and modeling benchmarks. *Journal of Climate*, 20(3), 449–469.

Charlton, A.J., Polvani, L.M., Perlwitz, J., Sassi, F., Manzini, E., Shibata, K., Pawson, S., Nielsen, J.E. & Rind, D., 2007. A New Look at Stratospheric Sudden Warmings. Part II: Evaluation of Numerical Model Simulations. *Journal of Climate*, 20(3), 470–488. doi: 10.1175/JCLI3994.1.

Charney, J.G. & Drazin, P.G., 1961. Propagation of planetary-scale disturbances from the lower into the upper atmosphere. *Journal of Geophysical Research*, 66(1), 83–109. doi: 10.1029/JZ066i001p00083.

Coughlin, K. & Gray, L.J., 2009. A Continuum of Sudden Stratospheric Warmings. *Journal of the Atmospheric Sciences*, 66(2), 531–540. doi: 10.1175/2008JAS2792.1.

Ebita, A., Kobayashi, S., Ota, Y., Moriya, M., Kumabe, R., Onogi, K., Harada, Y., Yasui, S., Miyaoka, K., Takahashi, K., Kamahori, H., Kobayashi, C., Endo, H., Soma, M., Oikawa, Y. & Ishimizu, T., 2011. The Japanese 55-year Reanalysis “JRA-55”: An Interim Report. *Sola*, 7, 149–152.

Gerber, E.P., Baldwin, M.P., Akiyoshi, H., Austin, J., Bekki, S., Braesicke, P., Butchart, N., Chipperfield, M., Dameris, M., Dhomse, S., Frith, S.M., Garcia, R.R., Garny, H., Gettelman, A., Hardiman, S.C., Karpechko, A., Marchand, M., Morgenstern, O., Nielsen, J.E., Pawson, S., Peter, T., Plummer, D. a., Pyle, J. a., Rozanov, E., Scinocca, J.F., Shepherd, T.G. & Smale, D., 2010. Stratosphere-troposphere coupling and annular mode variability in chemistry-climate models. *Journal of Geophysical Research*, 115, D00M06. doi: 10.1029/2009JD013770.

Gerber, E.P., Orbe, C. & Polvani, L.M., 2009. Stratospheric influence on the tropospheric circulation revealed by idealized ensemble forecasts. *Geophysical Research Letters*, 36(24), L24801. doi: 10.1029/2009GL040913.

Hannachi, A., Mitchell, D., Gray, L. & Charlton-Perez, A., 2011. On the Use of Geometric Moments to Examine the Continuum of Sudden Stratospheric Warmings. *Journal of the Atmospheric Sciences*, 68(3), 657–674. doi: 10.1175/2010JAS3585.1.

Hitchcock, P., Shepherd, T.G. & Manney, G.L., 2013. Statistical Characterization of Arctic Polar-Night Jet Oscillation Events. *Journal of Climate*, 26(6), 2096–2116. doi: 10.1175/JCLI-D-12-00202.1.

Hitchcock, P. & Simpson, I.R., 2014. The Downward Influence of Stratospheric Sudden Warmings. *Journal of the Atmospheric Sciences*, 71(10), 3856–3876. doi: 10.1175/JAS-D-14-0012.1.

Hu, J., Ren, R., Xu, H. & Yang, S., 2015. Seasonal timing of stratospheric final warming associated with the intensity of stratospheric sudden warming in preceding winter. *Science China Earth Sciences*, 58(4), 615–627. doi: 10.1007/s11430-014-5008-z.

Johnson, K.W., Miller, A.J. & Gelman, M., 1969. Proposed indices characterizing stratospheric circulation and temperature fields. *Monthly Weather Review*, 97, 565–570.

Karpechko, A.Y., Hitchcock, P., Peters, D.H.W. & Schneidereit, A., 2017. Predictability of downward propagation of major sudden stratospheric warmings. *Quarterly Journal of the*

Royal Meteorological Society, n/a--n/a. doi: 10.1002/qj.3017.

Kim, J., Son, S.-W., Gerber, E.P. & Park, H.-S., 2017. Defining Sudden Stratospheric Warming in Climate Models: Accounting for Biases in Model Climatologies. *Journal of Climate*, 0(0), null. doi: 10.1175/JCLI-D-16-0465.1.

Labitzke, K., 1981. Stratospheric-Mesospheric Midwinter Disturbances - a Summary of Observed Characteristics. *Journal of Geophysical Research-Oceans and Atmospheres*, 86(NC10), 9665–9678. doi: 10.1029/JC086iC10p09665.

Maury, P., Claud, C., Manzini, E., Hauchecorne, A. & Keckhut, P., 2016. Characteristics of stratospheric warming events during Northern winter. *Journal of Geophysical Research: Atmospheres*, 121(10), 5368–5380. doi: 10.1002/2015JD024226.

Maycock, A.C. & Hitchcock, P., 2015. Do split and displacement sudden stratospheric warmings have different annular mode signatures? *Geophysical Research Letters*, 42(24), 10,910-943,951. doi: 10.1002/2015GL066754.

McInturff, R.M., 1978. Stratospheric warmings: Synoptic, dynamic and general-circulation aspects. *Tech.Rep. NASA-RP-1017*, NASA Ref., 19.

Mitchell, D.M., Gray, L.J. & Charlton-Perez, a. J., 2011. The structure and evolution of the stratospheric vortex in response to natural forcings. *Journal of Geophysical Research*, 116(D15), D15110. doi: 10.1029/2011JD015788.

Palmeiro, F.M., Barriopedro, D., García-Herrera, R. & Calvo, N., 2015. Comparing Sudden Stratospheric Warming Definitions in Reanalysis Data. *Journal of Climate*. doi: 10.1175/JCLI-D-15-0004.1.

Quiroz, R.S., Miller, A.J. & Nagatani, R.M., 1975. A Comparison of Observed and Simulated

Properties of Sudden Stratospheric Warmings. *Journal of the Atmospheric Sciences*, 32(9), 1723–1736. doi: 10.1175/1520-0469(1975)032<1723:ACOOAS>2.0.CO;2.

Scherhag, R., 1952. Die explosionsartigen Stratosparenerwarmungen des Spatwinters 1952. *Ber. Det. Wetterdienstes (US Zone)*, 38, 51–63.

Seviour, W.J.M., Mitchell, D.M. & Gray, L.J., 2013. A practical method to identify displaced and split stratospheric polar vortex events. *Geophysical Research Letters*. doi: 10.1002/grl.50927.

Waugh, D.W. & Randel, W.J., 1999. Climatology of Arctic and Antarctic Polar Vortices Using Elliptical Diagnostics. *Journal of the Atmospheric Sciences*, 56(11), 1594–1613. doi: 10.1175/1520-0469(1999)056<1594:COAAAP>2.0.CO;2.

WMO/IQSY, 1964. International Years of the Quiet Sun (IQSY) 1964-65. Alert messages with special references to stratwarms. WMO/IQSY Report No 6, Secretariat of the World Meteorological Organization, Geneva, Switzerland.

WMO CAS, 1978. WMO Commission for Atmospheric Sciences, Abridged Final Report of the Seventh Session, Manila, 27 February-10 March 1978. WMO- No. 509. (p. 36, item 9.4.4).

Figure Captions

Figure 1. (a,b) The mean zonal wind tendency at 10 hPa 60°N for days 0-5 *after* each reversal minus days 5-15 *prior* to each reversal; and (c, d) the mean temperature anomaly at 10 hPa 50-90°N for days -5 to +5 of each reversal, as a function of latitude and (a,c) pressure level (with a threshold of 0 m s^{-1}) and (b,d) threshold (at 10 hPa). Thin white contours in (a,c) show the mean DJFM zonal winds at 3 m s^{-1} intervals, with the highest contour near 50-60°N at 1 hPa equal to 39 m s^{-1}. Stippling indicates where values are *not* significant based on Monte Carlo testing (see details in **Section 2**).

Figure 2. (a,b) The mean eddy heat flux anomaly at 100 hPa and 45-75°N for days 20-0 *prior* to each reversal; and (c, d) the mean daily Arctic Oscillation index (standardized by the DJFM mean) for days 0-60 after each reversal, as a function of latitude and (a,c) pressure level (with a threshold of 0 m s^{-1}) and (b,d) threshold (at 10 hPa). Thin white contours in (a,c) show the mean DJFM zonal winds at 3 m s^{-1} intervals, with the highest contour near 50-60°N at 1 hPa equal to 39 m s^{-1}. Stippling indicates where values are *not* significant based on Monte Carlo testing (see details in **Section 2**).

Figure 3. (a,b) The frequency or number of SSWs per decade; and (c, d) the percent match of SSW dates at a given location with SSW dates at 60°N, 10 hPa, and a 0 m s^{-1} threshold. Thin white contours in (a) show the mean DJFM zonal winds at 3 m s^{-1} intervals, with the highest contour near 50-60°N at 1 hPa equal to 39 m s^{-1}. Black contour in (b) indicates where there are

fewer than 2 SSWs per decade; black contour in (c,d) indicates where date agreement is higher than 50%.

Figure 4. The average of all the metric scores, defined as the metric at each location divided by the maximum metric, as a function of latitude and (a) pressure level (with a threshold of 0 m s^{-1}) and (b) threshold (at 10 hPa). Thin white contours in (a) show the mean DJFM zonal winds at 3 m s^{-1} intervals, with the highest contour near 50-60°N at 1 hPa equal to 39 m s^{-1}. Solid black line indicates where the metric score exceeds 0.8.

Table 1. Major SSWs in the Northern Hemisphere defined by reversals of the zonal wind at 60°N and 10 hPa, for this study (left column) and for CP07 (right column). The last row shows the total number of SSWs.

Major SSWs, This study	**Major SSWs, CP07**
30-Jan-58	30-Jan-58
17-Jan-60	17-Jan-60
30-Jan-63	30-Jan-63
18-Dec-65	18-Dec-65
23-Feb-66	23-Feb-66
7-Jan-68	7-Jan-68
29-Nov-68	29-Nov-68
2-Jan-70	2-Jan-70
18-Jan-71	18-Jan-71
20-Mar-71	20-Mar-71
31-Jan-73	31-Jan-73
9-Jan-77	9-Jan-77
22-Feb-79	22-Feb-79
29-Feb-80	29-Feb-80
6-Feb-81	6-Feb-81
--	4-Mar-81
4-Dec-81	4-Dec-81
24-Feb-84	24-Feb-84
1-Jan-85	1-Jan-85
23-Jan-87	23-Jan-87
8-Dec-87	8-Dec-87
FW	14-Mar-88
21-Feb-89	21-Feb-89
15-Dec-98	15-Dec-98
26-Feb-99	26-Feb-99
20-Mar-00	20-Mar-00
11-Feb-01	11-Feb-01
31-Dec-01	31-Dec-01
18-Jan-03	18-Jan-03
5-Jan-04	5-Jan-04
21-Jan-06	21-Jan-06
24-Feb-07	24-Feb-07
22-Feb-08	22-Feb-08
24-Jan-09	24-Jan-09
9-Feb-10	9-Feb-10
--	24-Mar-10
7-Jan-13	7-Jan-13
34	**37**

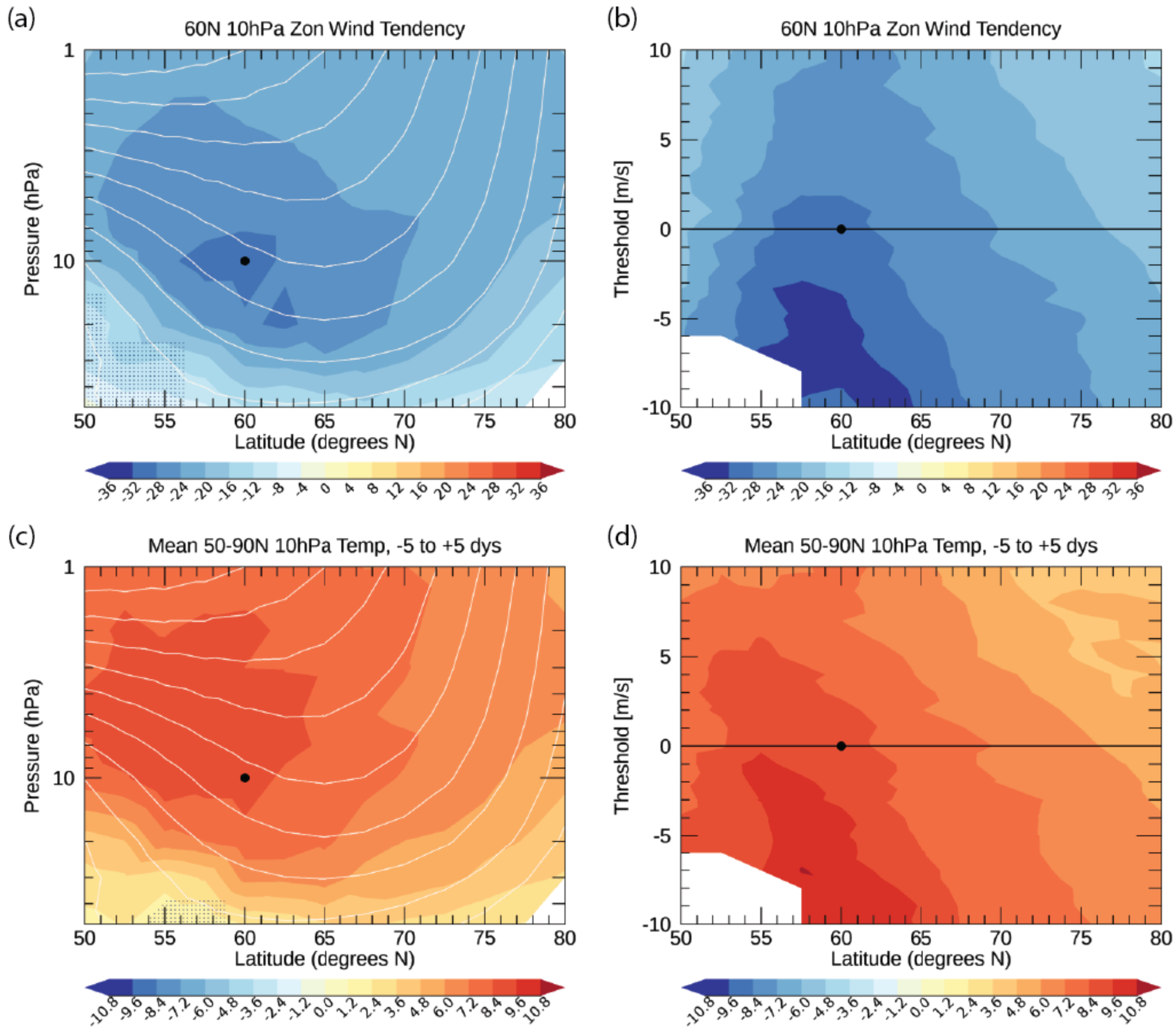

Figure 1. (a,b) The mean zonal wind tendency at 10 hPa 60°N for days 0-5 *after* each reversal minus days 5-15 *prior* to each reversal; and (c, d) the mean temperature anomaly at 10 hPa 50-90°N for days -5 to +5 of each reversal, as a function of latitude and (a,c) pressure level (with a threshold of 0 m s^{-1}) and (b,d) threshold (at 10 hPa). Thin white contours in (a,c) show the mean DJFM zonal winds at 3 m s^{-1} intervals, with the highest contour near 50-60°N at 1 hPa equal to 39 m s^{-1}. Stippling indicates where values are *not* significant based on Monte Carlo testing (see details in **Section 2**).

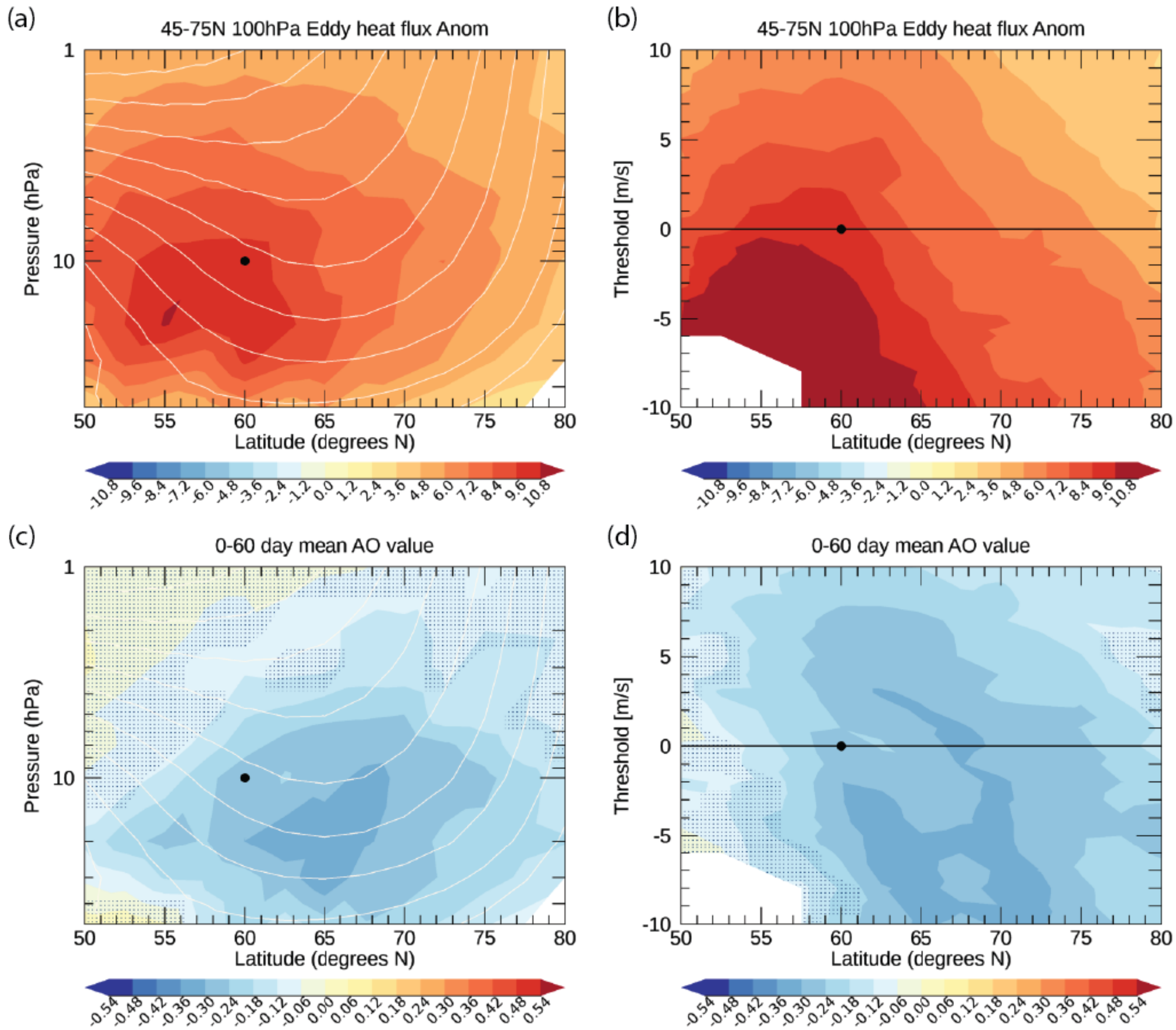

Figure 2. (a,b) The mean eddy heat flux anomaly at 100 hPa and 45-75°N for days 20-0 *prior* to each reversal; and (c, d) the mean daily Arctic Oscillation index (standardized by the DJFM mean) for days 0-60 after each reversal, as a function of latitude and (a,c) pressure level (with a threshold of 0 m s^{-1}) and (b,d) threshold (at 10 hPa). Thin white contours in (a,c) show the mean DJFM zonal winds at 3 m s^{-1} intervals, with the highest contour near 50-60°N at 1 hPa equal to 39 m s^{-1}. Stippling indicates where values are *not* significant based on Monte Carlo testing (see details in **Section 2**).

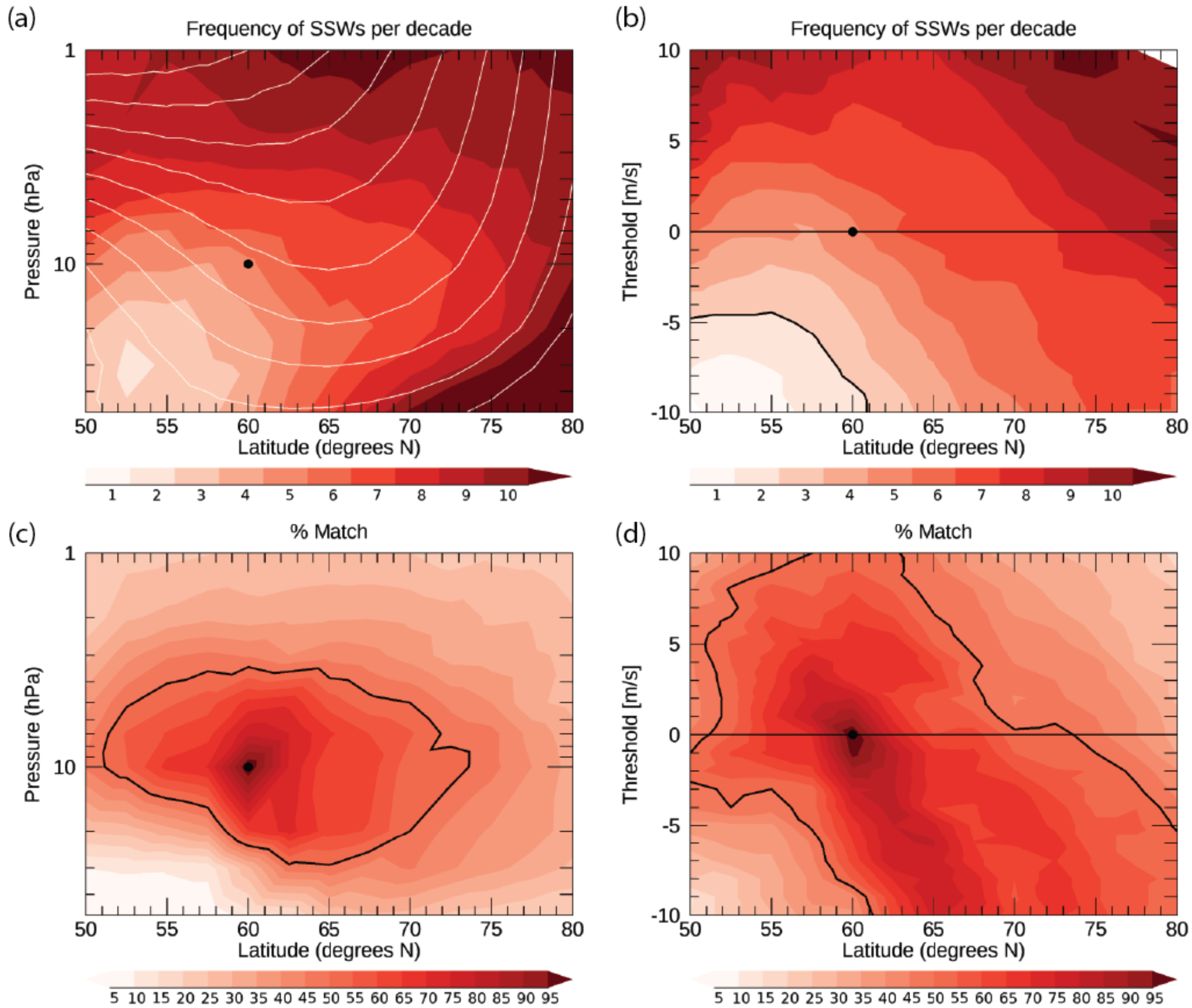

Figure 3. (a,b) The frequency or number of SSWs per decade; and (c, d) the percent match of SSW dates at a given location with SSW dates at 60°N, 10 hPa, and a 0 m s^{-1} threshold. Thin white contours in (a) show the mean DJFM zonal winds at 3 m s^{-1} intervals, with the highest contour near 50-60°N at 1 hPa equal to 39 m s^{-1}. Black contour in (b) indicates where there are fewer than 2 SSWs per decade; black contour in (c,d) indicates where date agreement is higher than 50%.

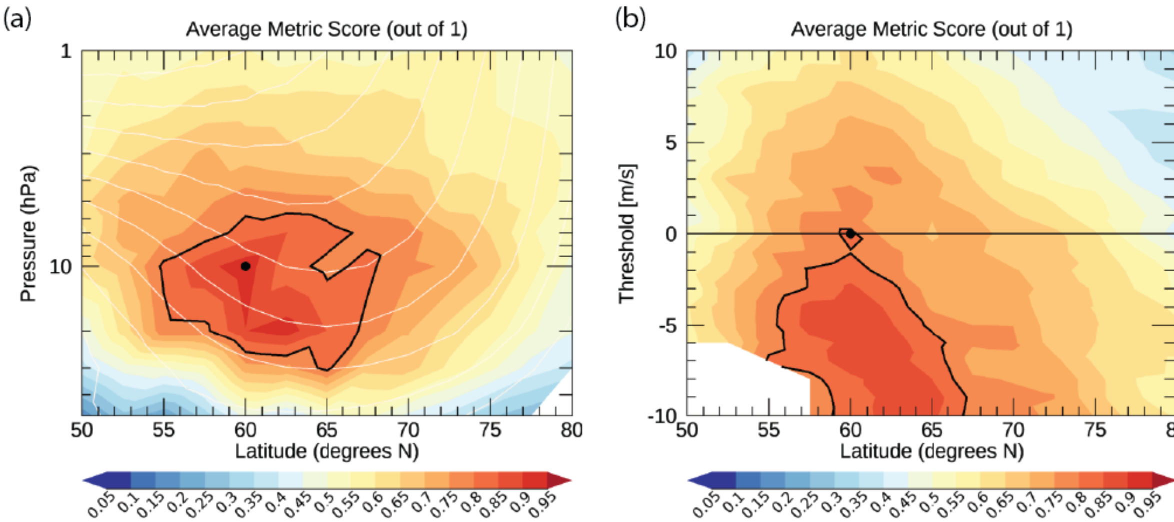

Figure 4. The average of all the metric scores, defined as the metric at each location divided by the maximum metric, as a function of latitude and (a) pressure level (with a threshold of 0 m s^{-1}) and (b) threshold (at 10 hPa). Thin white contours in (a) show the mean DJFM zonal winds at 3 m s^{-1} intervals, with the highest contour near 50-60°N at 1 hPa equal to 39 m s^{-1}. Solid black line indicates where the metric score exceeds 0.8.